Journal of Heat and Mass Transfer Research

Journal homepage: https://jhmtr.semnan.ac.ir

Semnan University

ISSN: 2383-3068

Research Article

Numerical Studies on the Effect of Different Obstruction Geometries on Performance of Rectangular Channel Air Heaters

Bronin Cyriac [a]*, Siddappa S. Bhusnoor [b]

[a] *Department of Mechanical Engineering, K J Somaiya College of Engineering, Mumbai-400077, India.*

[b] *Department of Mechanical Engineering, K J Somaiya College of Engineering, Somaiya Vidyavihar University, Mumbai-400077, India.*

ARTICLE INFO

Article history:

Received: 2023-03-28

Revised: 2024-01-27

Accepted: 2024-01-27

Keywords:

Air heater,

Thermal enhancement factor;

Artificial roughness;

Flow obstruction;

Turbulence;

ABSTRACT

Air heaters have poor thermal efficiency. Flow obstructions improve the efficiency of the air heater by enhancing heat transfer and disrupting the formation of the laminar sub-layer. In the present study, a rectangular channel of aspect ratio 6 and obstructions of various geometry (triangular, rectangular, and arc (or semi-circular)) are used with a longitudinal pitch (P_l/e) of 4, transverse pitch (P_t/b) of 2 ratios for Reynolds Number (Re) from 5000 to 20000. Various performance parameters such as Nusselt Number (Nu), Friction factor (f), and Thermal Enhancement Factor (TEF) were analyzed for the above conditions using Computational Fluid Dynamics (CFD) to compare the thermohydraulic performance of air heaters with various obstruction geometries. Maximum TEF of 1.27, 1.08, and 1.05 are obtained at Re = 5000 for delta, rectangular, and arc flow obstructions, respectively. Delta flow obstructions are superior to arc and rectangular shapes for the investigated range of Reynolds numbers.

1. Introduction

The rising demand for energy worldwide is leading to increased use and reliance on non-renewable energy sources [1]. The environment and human health are suffering due to the rapid depletion of conventional energy sources and the growing energy demand. Researchers are trying to improve the energy efficiency of thermal systems due to these issues [2]. The growing significance of renewable energy also comes with its inherent challenges. Various researchers underscored challenges like the unpredictability of the energy source, intermittency, and relatively low energy density [3]. Also, the increasing global energy demand and the depletion of fossil fuel fuels have raised questions about the reliability of renewable energy sources [4]. Researchers have studied the impact of various factors on greenhouse gas emissions [5]. The rapid depletion of fossil fuel reserves, constituting 79% of global energy sources with a significant 57% allocated to transportation, raises concerns about economic stability. This scenario emphasizes the criticality of transitioning to local and sustainable energy sources [6]. Governments worldwide are focused on fighting global warming by transitioning toward renewable energy [7].

Solar air collectors harness solar energy directly and heat air without relying on electricity

* **Corresponding author.**
E-mail address: bronin.cyriac@gmail.com

Cite this article as:
Cyriac, B., and Bhusnoor, S. S., 2024. Numerical Studies on the Effect of Different Obstruction Geometries on Performance of Rectangular Channel Air Heaters. *Journal of Heat and Mass Transfer Research*, 11(1), pp. 43 - 52.
https://doi.org/10.22075/JHMTR.2023.39315.2050

[8]. Solar energy holds promise for substituting conventional power sources. The solar air heater (SAH) captures solar radiation, converting it into thermal energy [8]. The heat transfer properties of an air heater are increased by adding artificial surface roughness to the absorber plate [9,10]. Artificial surface roughness in the form of winglets [11,12], ribs [13,14], and perforated and non-perforated obstructions [15,16] improve the heat transfer coefficient (h) of air by producing turbulence in the laminar sublayer [17,18]. This also creates an additional pressure drop in the system [19]. The improvement in heat transfer and the increase in friction factor must be considered to evaluate the effectiveness of a flow obstruction. The connective heat transfer obtained after employing flow obstruction cannot be compared directly with the convective heat transfer coefficient (h) of a smooth air heat as the blower will be consuming to maintain the same flow condition. Webb and Han [20,21] to decide whether the surface roughness is potentially beneficial or not [22]. This criterion allows for a more nuanced evaluation by normalizing the heat transfer enhancement of the air heater's enhanced surface against the smooth channel under equivalent blowing power conditions.

$$TEF = \left(\frac{Nu}{Nu_o}\right)\left(\frac{f}{f_o}\right)^{\frac{-1}{3}} \quad (1)$$

Where Nu/Nu_o is the ratio of the Nusselt number of the air heater with the roughed surface to that of the smooth surface, similarly, f/f_o is the ratio of the friction factor of the air heater with a roughened surface to that of a smooth surface. A TEF value greater than one is required for an obstruction to be effective.

Prior studies have documented the impact of different geometries on improving heat transfer, yet there exists a paucity of research comparing the effect of distinct geometrical shapes. This investigation uses numerical techniques to examine the thermo-hydraulic features of an air heater with flow obstructions of delta, arc, and rectangular shapes.

2. Numerical modelling of air heater

For the analysis of different flow obstructions' thermo-hydraulic properties, an air heater of size 1200 mm × 300mm × 50 mm was selected. Using CFD, the air heater was evaluated for various flow rates by placing the flow obstructions vertically in the flow field (i.e., $\alpha = 90^o$). The relative obstruction height (e/H = 0.5), relative obstruction longitudinal pitch (P_l/e = 4), and relative obstruction transverse pitch (P_t/b = 2) were kept constants for all the geometries.

TEF was calculated to assess the effectiveness of obstructions in enhancing the air heater's thermal performance with minimum impact on its hydraulic performance. The computational domain was designed for only one transverse pitch length (P_t), as illustrated in Fig. 1, with only one column of obstructions being considered to take advantage of the domain's periodicity. The symmetry boundary condition was applied on one side. Patankar et al. [23] proposed the periodic boundary condition solution procedure to simulate the flow. The concept of periodic boundary conditions allows for the confinement of flow field analysis to a single isolated module without considering the entrance region [24, 25]. A wall boundary condition was applied on the bottom surface with a constant heat flux (800 W/m^2). The boundary conditions used in the numerical simulations were designed to accurately represent the physical behavior of the air in the air heater. A wall boundary condition was applied to ensure the no-slip condition on all surfaces. The thermophysical properties of air were also considered, considering an input temperature of 300 K. The computational domain was discretized by utilizing an unstructured tetrahedron mesh, complemented by a prism mesh at the boundary. This mesh generation method was selected to ensure that the domain discretization is optimized for accurately capturing the flow features while minimizing computational resources. Additionally, the prism mesh at the boundary was applied to enhance the accuracy of the solution near the walls, as the flow near the walls is highly influenced by the surface conditions.

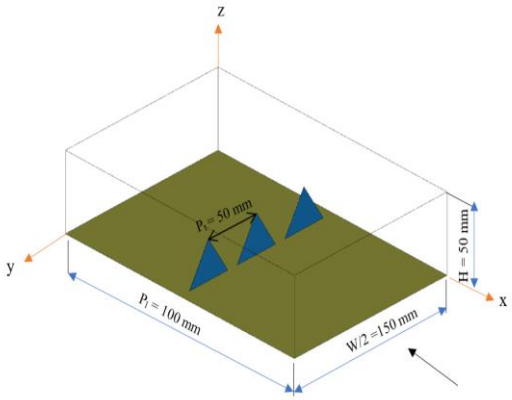

Fig. 1. Computational domain for the numerical analysis of air heater with obstruction

The delta, rectangular, and arc obstructions were modeled as demonstrated in Fig. 2, corresponding to one longitudinal pitch length (P_l). Constant values were considered for the relative obstruction height (e/H =0.5), relative obstruction longitudinal pitch (P_l/e = 4), and relative obstruction transverse pitch (P_t/b = 2)

for all the geometries. The models, methods, and convergence criteria utilized for the CFD modeling are listed in Table 1.

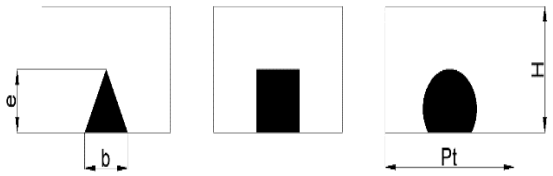

Fig. 2. Various geometries of the obstruction for numerical study (delta, rectangle, and arc)

Table 1. Computational Fluid Dynamics (CFD) modelling of air heater

Parameter	Model/ Condition
Flow modelling	Navier-Stokes Eq.
Pressure Velocity coupling	COUPLED algorithm
Turbulence modelling	k-ε turbulence model with enhanced wall treatment
Convergence Condition	Continuity, Velocity, turbulence dissipation terms: 10^{-3} Energy: 10^{-6}
Spatial discretisation	QUICK scheme

2.1. Validation of the Numerical Model

Results from the numerical simulation were compared with those calculated using empirical correlations (Eq. 2, Eq. 3) and experimental data published in previous studies [22, 26-28], as shown in Fig. 3 and Fig. 4. CFD results are in a descent agreement with empirical correlations. The average deviation of the Nu and f from CFD with empirical correlations (Dittus–Boelter Equation (Eq. 2) and Modified Blasius Equation (Eq. 3) [29] are 5.68% and 7.2%, respectively. Also, the results closely matched the other published experimental results.

$$Nu = 0.023\, Re^{0.8}\, Pr^{0.4} \quad (2)$$

$$f = 0.085\, Re^{-0.25} \quad (3)$$

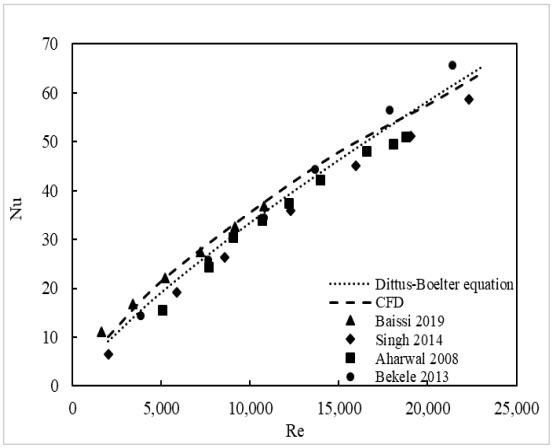

Fig. 3. Variation of Nu with Re for smooth duct

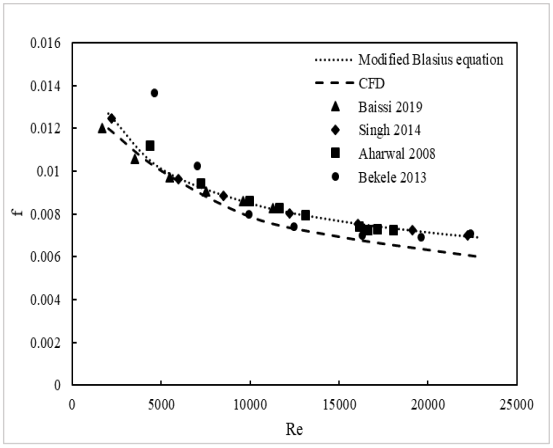

Fig. 4. Variation of friction factor with Re for smooth duct

3. Results and Discussion

The following sub-sections discuss the effect of triangular (delta), arc, and rectangular-shaped flow obstructions on performance parameters Nu, f, and TEF.

3.1. Effect of Obstruction Geometry on the Flow Behaviour of Air Heater

Turbulence intensity generated by different obstruction geometries on the heated surface is given in Table 2. The turbulence intensity values indicate the extent of turbulence produced by each geometry at varying Reynolds numbers (Re) ranging from 5000 to 20000.

Table 2. Turbulence intensity produced various obstruction geometries near the heated surface.

Geometry	Blockage ratio A_{ob} /A (%)	Turbulence Intensity (%)			
		5000	10000	15000	20000
Smooth	1	0.3	0.9	1.9	3
Delta	1.25	8.5	18.6	27.8	37.6
Rectangle	2.5	10.4	22.3	35.1	51.4
Arc	2.6	10.3	22.6	35.6	51.8

The rectangular and arc obstructions substantially improve the turbulence intensity in the investigated range of Re. The high turbulence intensity induced by the obstructions can be attributed to the high blockage ratio of these obstructions. Blockage ratio (A_{ob}/A) is defined as the ratio of the obstructed area (A_{ob}) created by the obstruction geometry to the total cross-sectional area (A) through which the fluid flows. It quantifies the degree of flow obstruction imposed by the geometric configuration. Arc and rectangular obstructions produce higher blockage ratios compared to delta obstructions. This indicates that arc and rectangular obstructions significantly impede the flow by occupying a larger proportion of the cross-sectional area. This results in the creation of enhanced turbulence levels near the heated surface. Because of the improved turbulence produced by the rectangular flow obstructions, the flow velocity increases, as seen in the velocity contour plot given in Fig. 5. This improved velocity ultimately results in improved heat transfer and enhanced heat removal from the heated surface, as visible from the temperature contour plot in Fig. 8.

The implementation of flow obstructions with different shapes on the flow field was observed to generate vortices, consequently enhancing turbulence intensity downstream, as illustrated in Fig. 5. This phenomenon results in improved heat transfer by the flow obstructions. The delta obstructions were found to cause the least flow disturbance, while the rectangular obstructions caused the maximum disturbance. Figure 6 indicates that the rectangular flow obstructions produced the highest turbulence intensity. The improved turbulence generated by the rectangular flow obstructions increases the flow velocity (Fig. 7), ultimately enhancing heat transfer from the bottom surface, as depicted in Fig. 8.

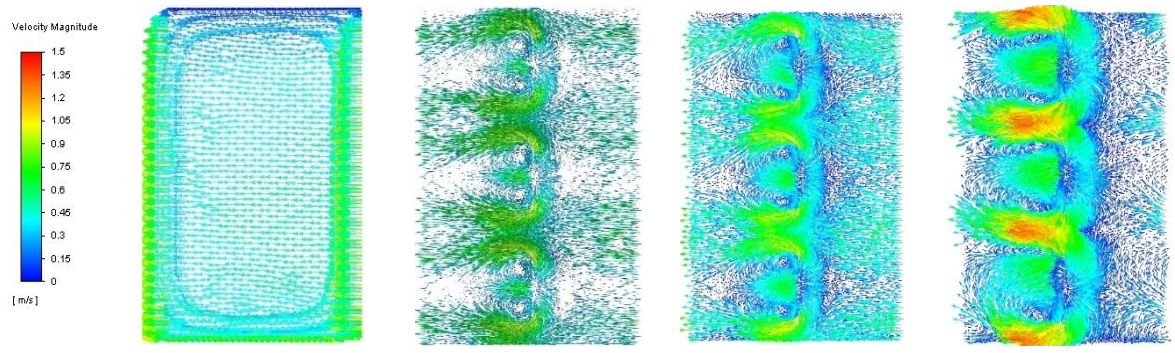

Fig. 5. Velocity vector on an imaginary plane 1 mm above the bottom surface of the air heater with (a) smooth, (b) delta, (c) arc and (d) rectangular flow obstructions (Re =5000)

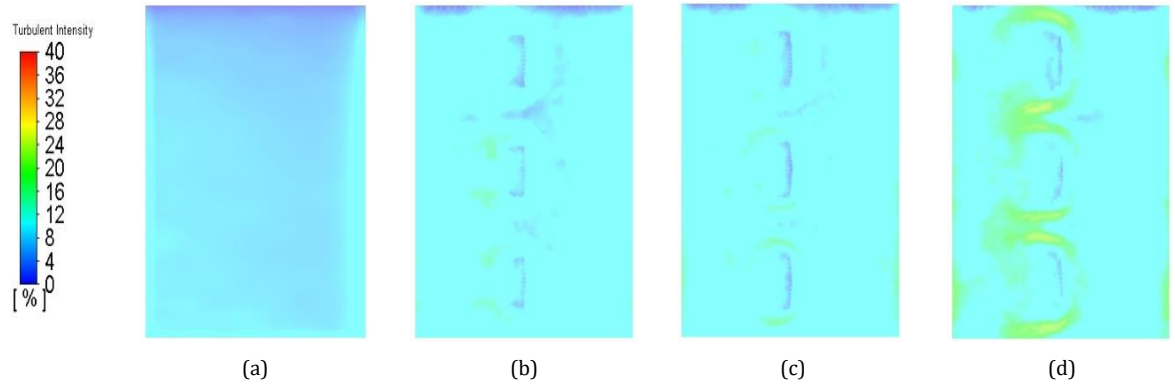

Fig. 6. Turbulent intensity contour on an imaginary plane 1 mm above the bottom surface of an air heater with (a) smooth, (b) delta, (c) arc and (d) rectangular flow obstructions (Re =5000)

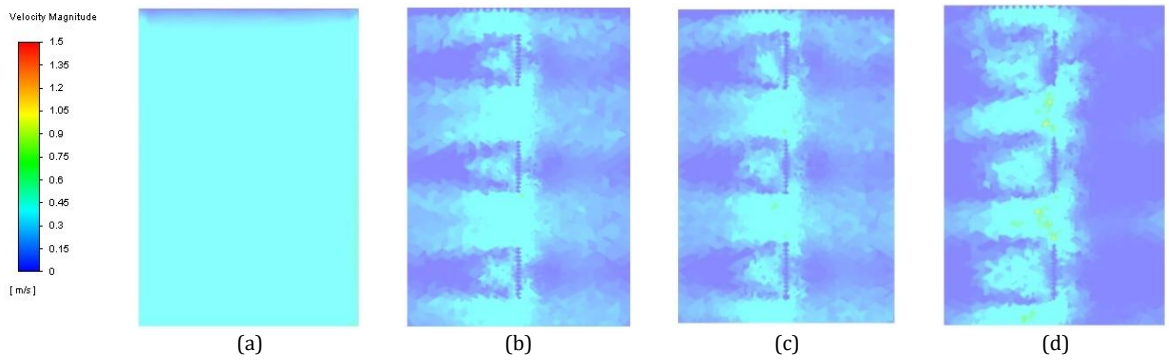

Fig. 7. Velocity contour on an imaginary plane 1 mm above the bottom surface of the air heater with (a) smooth, (b) delta, (c) arc and (d) rectangul*ar* flow obstructions *(Re =5000)*

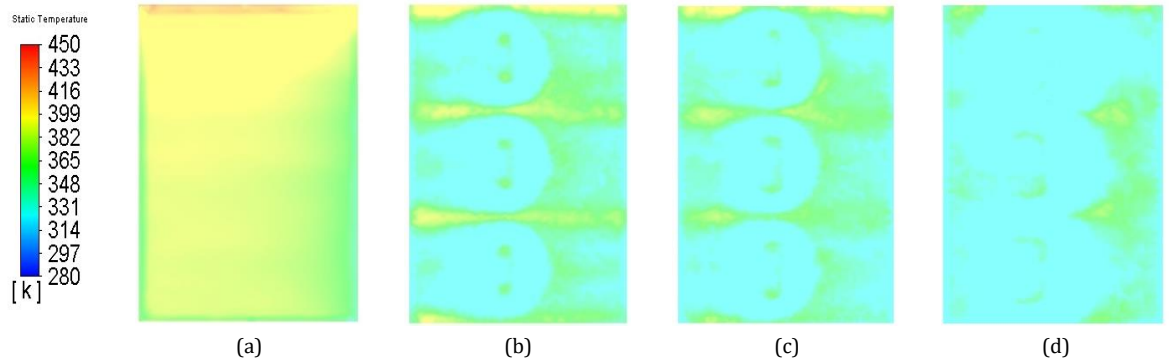

Fig. 8. Temperature contour on an imaginary plane 1 mm above the bottom surface of the air heater with (a) smooth, (b) delta, (c) arc and (d) rectangul*ar flow obstructions (Re =5000)*

The pathlines on the air heater's bottom surface and the velocity vectors on the mid-plane parallel to the side surface are depicted in Figures 9 and 10. At a Reynolds number of 15000, these graphs illustrate the turbulence produced by the delta flow obstructions.

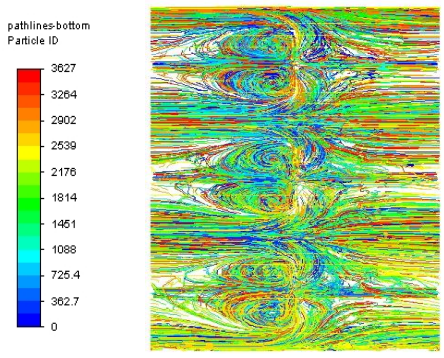

Fig. 9. Pathlines o*n the bottom surface of the air* heater with delta flow obstructions

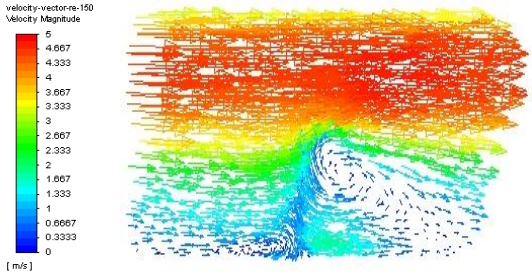

Fig. 10. Velocity vector on the bottom surface of the air heater with delta flow obstructions *(Re =5000)*

3.2. Effect of Obstruction Geometry on Thermal Performance Parameters of the Air Heater

The effect of the delta, rectangular and arc obstructions on Nu was analysed, and the results are discussed using Fig. 11.

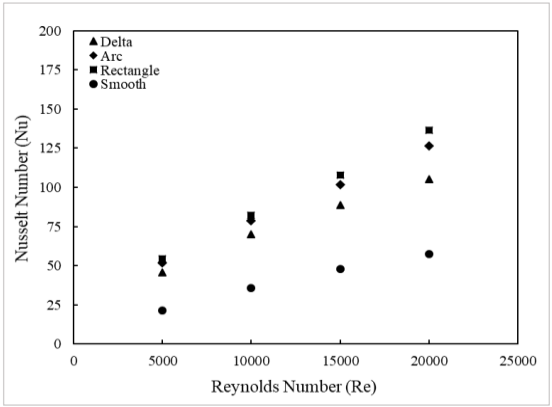

Fig. 11. Effects of Obstruction Geometry on Thermal Performance of an Air Heater at Varying Fluid Flow Rates

The air heater's Nusselt number (Nu) consistently increases with the increase in Reynolds number (Re) for all types of obstructions, primarily attributed to turbulence amplification within the flow. Among different obstruction shapes, both rectangular and arc configurations manifest notable increases in Nu enhancement (represented as the ratio of Nu

with obstruction to Nu without obstruction) across the entire range of Reynolds numbers, as presented in Table 3. This enhancement directly results from the increased turbulence intensity generated by these obstructions.

Delta obstructions exhibit an enhancement range of 1.83 to 2.14, reflecting their moderate influence on turbulence. Arc obstructions demonstrate an even more substantial influence, yielding an enhancement range of 2.1 to 2.4. However, the rectangular obstructions stand out by achieving the highest Nu enhancement range of 2.3 to 2.53. Rectangular obstructions exhibit the most substantial increase in Nusselt number (Nu) enhancement, reaching a value of 2.53 at a Reynolds number (Re) of 5000. This result underscores the significant impact of rectangular obstruction geometry in enhancing heat transfer within the air heater.

3.3. Effect of Obstruction Geometry on Hydraulic Performance Parameters of the Air Heater

The impact of delta, rectangular, and arc obstructions on f was studied using numerical techniques, and the outcomes are illustrated in Fig. 12.

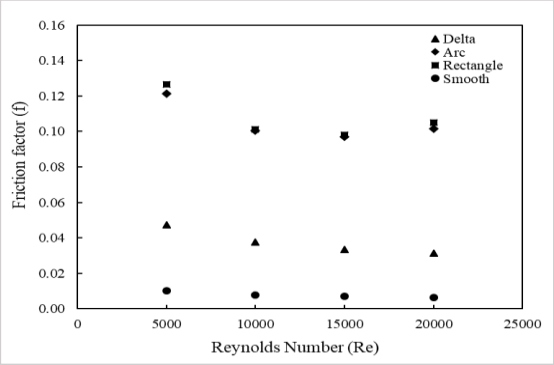

Fig. 12. Effects of Obstruction Geometry on Hydraulic Performance of an Air Heater at Varying Fluid Flow Rates

The air heater's Nusselt number (Nu) consistently increases with the increase in Reynolds number (Re) for all types of obstructions, primarily attributed to turbulence amplification within the flow. Among different obstruction shapes, both rectangular and arc configurations manifest notable increases in Nu enhancement (represented as the ratio of Nu with obstruction to Nu without obstruction) across the entire range of Reynolds numbers, as presented in Table 3. This enhancement directly results from the increased turbulence intensity generated by these obstructions.

Delta obstructions exhibit an enhancement range of 1.83 to 2.14, reflecting their moderate influence on turbulence. Arc obstructions demonstrate an even more substantial influence, yielding an enhancement range of 2.1 to 2.4. However, the rectangular obstructions stand out by achieving the highest Nu enhancement range of 2.3 to 2.53. Rectangular obstructions exhibit the most substantial increase in Nusselt number (Nu) enhancement, reaching a value of 2.53 at a Reynolds number (Re) of 5000. This result underscores the significant impact of rectangular obstruction geometry in enhancing heat transfer within the air heater.

As observed from Fig. 12, the flow obstruction creates more pressure drop (f) and flow detachment. The f for all obstructions decreases with Re due to the decrease in residence time of air with the heated surface. Also, reattachment distance increases the recirculation zone behind the obstruction. Because of the more considerable pressure drop caused by this, f for air heaters with obstructions rises. f augmentation is least for delta obstruction as delta offers minimum flow blockage. f augmentation (fobstruction/fsmooth) is the least for delta obstruction as delta offers minimum flow blockage. The friction factor augmentation is minimum for Re = 5000 and maximum for Re = 20,000. The friction factor augmentation (fobstruction / fsmooth) varies between 4.7 to 4.9 for delta obstructions, and the friction factor augmentation varies between 12 to 16 for rectangular and arc obstructions.

Table 3. Nusselt number enhancement and friction factor augmentation produced by various obstruction geometries for various flow rates.

Type of Obstruction		Reynolds Number			
		5000	10000	15000	20000
Delta	Nu/ Nu_o	2.14	1.97	1.85	1.83
	f/ f_o	4.73	4.75	4.79	4.92
Rectangle	Nu/ Nu_o	2.53	2.31	2.25	2.37
	f/ f_o	12.64	12.83	14.11	16.56
Arc	Nu/ Nu_o	2.41	2.21	2.12	2.2
	f/ f_o	12.1	12.74	13.95	16.01

3.4. Effect of Obstruction Geometry on Thermo-Hydraulic Performance Parameters of the Air Heater

The influence of the type of geometry of the obstruction (delta, rectangular, and arc) on TEF as a function of Re is shown in Fig. 13.

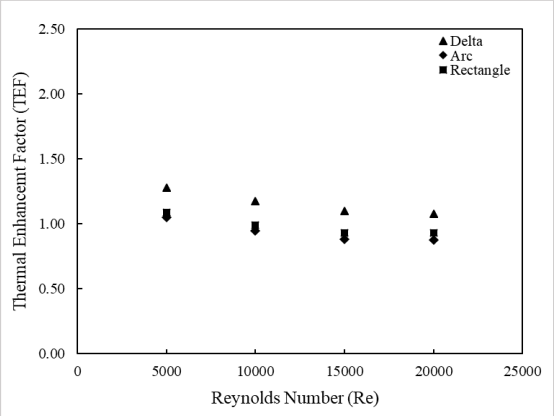

Fig. 13. Effects of Obstruction Geometry on Thermo-Hydraulic Performance of an Air Heater at Varying Fluid Flow Rates

The Thermal Enhancement Factor (TEF) was examined for delta, arc, and rectangular obstructions across the investigated range of Reynolds numbers (Re). The delta obstruction yields a TEF varying from 1.07 to 1.27, signifying an improved thermal performance compared to a smooth duct. The highest TEF of 1.27 was obtained at Re of 5000. The arc obstruction produces a TEF ranging from 0.9 to 1.08, while the rectangular obstruction presents a TEF ranging from 0.87 to 1.05 in the investigated range of Re.

A comparison of TEF values shows that the delta obstructions perform better than both arc and rectangular obstructions in enhancing the thermo-hydraulic performance of the air heater in the studied range of Reynolds number. This finding underscores the potential benefits of employing delta-shaped obstructions in improving the efficiency of the air heater. Even though rectangular obstructions create high Nu enhancement (Nu/Nu_o), the high f augmentation (f/f_o) associated with the rectangular obstruction reduces its TEF. At the same time, low f augmentation helps delta obstructions to create better TEF.

Fig. 14 and Fig. 15 represent the Nusselt number (Nu) and friction factor (f) data for the air heater with delta flow obstructions in comparison with the results from the previously published works [30-33].

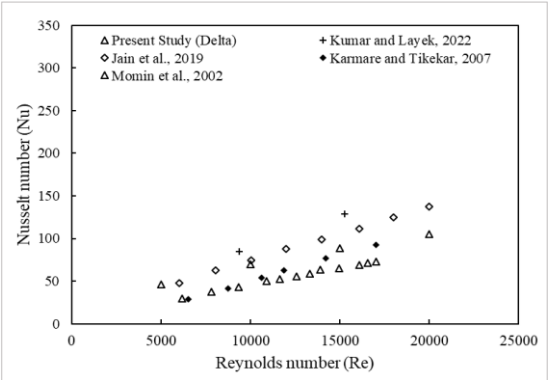

Fig. 14. Effect of Re on Nu of an air heater with delta flow obstruction along with other published results.

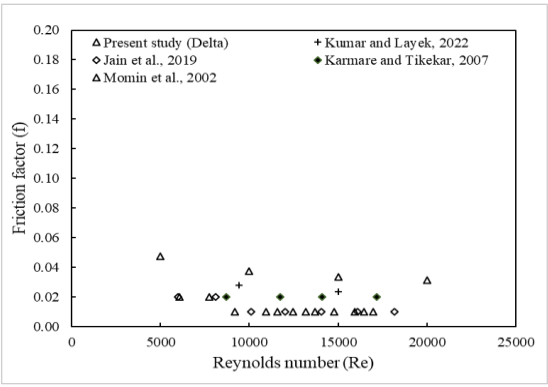

Fig. 15. Effect of Re on f of an air heater with delta flow obstruction along with other published results.

4. Conclusions

A numerical analysis of the air heater with delta, arc, and rectangular flow obstructions was conducted using CFD. Summary of the findings of the current investigation are listed below.

- The incorporation of flow obstructions yields substantial improvements in air heater performance, often coupled with discernible pressure differentials.
- As the air flow rate (Re) increases, the Nusselt number (Nu) reduces, while the friction factor (f) decreases for all types of flow obstructions due to the increased turbulence intensity at higher flow rates (Fig. 9, Fig. 10).
- The Nusselt number enhancement is significantly higher for rectangular obstructions than for other shapes for the entire range of Reynolds numbers. Rectangular obstruction provides Nu enhancement of 2.53 at Re=5000.
- The friction factor augmentation varies between 4.7 and 4.9 for delta obstructions, and the friction factor augmentation varies between 12 and 16 for rectangular and arc obstructions.

- The delta flow obstructions are superior to arc and rectangular shapes in improving air heater performance. Maximum TEF of 1.27, 1.08 and 1.05 are obtained at Re 5000 for delta, rectangular and arc flow obstructions, respectively.
- Delta flow obstructions are found to be superior to arc and rectangular shapes in improving the Thermo-Hydraulic performance of air heaters. The effect of inclination, blockage ratios, perforation and pitch of the delta flow obstruction on the performance of the air heater can be studied in future.

Nomenclature

A	Crosssectional area of air heater (m^2)
A_{ob}	Area obstructed by the flow flow obstruction (m^2)
A_{ob} / A	Blockage ratio
b	Base width of obstruction (mm)
CFD	Fluid Dynamics
e	Height of obstruction (mm)
e/H	Relative Obstruction Height
f	Friction factor of the surface with obstruction
f_o	Friction factor of the surface without obstruction
H	Height of air heater (mm)
h	Convective heat transfer of the enhanced surface (W/m^2K)
h_o	Convective heat transfer of the smooth surface (W/m^2K)
Nu	Nusselt number of the surface with obstruction
Nu_o	Nusselt number of the surface without obstruction
P_l	Longitudinal pitch (m)
P_l/e	Relative obstruction longitudinal pitch
P_t	Transverse pitch (m)
P_t/b	Relative obstruction transverse pitch
Q_s	Heat supplied to air (W)
QUICK	Quadratic Upstream Interpolation for Convective Kinematics
Re	Reynolds number
TEF	Thermal Enhancement Factor (ratio of enthalpy of the air heater with flow obstruction to the enthalpy of the air heater without flow obstruction at identical blowing power)
W	Width of air heater (mm)

Funding Statement

This research did not receive any specific grant from funding agencies in the public, commercial, or not-for-profit sectors.

Conflicts of Interest

The authors have no conflicts of interest to declare.

References

[1] Yadav, A.S. and Thapak, M.K., 2016. Artificially roughened solar air heater: A comparative study. *International Journal of Green Energy, 13(2)*, pp. 143-172. doi: 10.1080/15435075.2014.917419.

[2] Kumar, M., Sansaniwal, S.K. and Khatak, P., 2016. Progress in solar dryers for drying various commodities. *Renewable and Sustainable Energy Reviews, 55*, pp.346-360. doi: 10.1016/j.rser.2015.10.158.

[3] Shayan, M.E., Najafi, G., Ghobadian, B., Gorjian, S. and Mazlan, M., 2023. A novel approach of synchronization of the sustainable grid with an intelligent local hybrid renewable energy control. *International Journal of Energy and Environmental Engineering, 14(1)*, pp.35-46. doi: 10.1007/s40095-022-00503-7.

[4] Esmaeili Shayan, M., Najafi, G. and Esmaeili Shayan, S., 2023. Energy Management Model for a Standalone Hybrid Microgrid Using a Dynamic Decision-Making Algorithm. Amirkabir *Journal of Mechanical Engineering, 55(1)*, pp.3-20. doi: 10.22060/mej.2023.20755.7346.

[5] Esmaeili Shayan, M., Najafi, G., Ghobadian, B., Gorjian, S., Mazlan, M., Samami, M. and Shabanzadeh, A., 2022. Flexible photovoltaic system on non-conventional surfaces: a techno-economic analysis. Sustainability, 14(6), p.3566. doi: 10.3390/su14063566.

[6] Shayan, M.E., Najafi, G., Ghobadian, B., Gorjian, S., Mamat, R. and Ghazali, M.F., 2022. Multi-microgrid optimization and energy management under boost voltage converter with Markov prediction chain and dynamic

decision algorithm. Renewable Energy, 201, pp.179-189. doi: 10.1016/j.renene.2022.11.006.

[7] Shayan, M.E., Najafi, G. and Lorenzini, G., 2023. Optimization of a dual fuel engine based on multi-criteria decision-making methods. *Thermal Science and Engineering Progress, 44*, p.102055. doi: 10.1016/j.tsep.2023.102055.

[8] Shayan, M.E., Ghasemzadeh, F. and Rouhani, S.H., 2023. Energy storage concentrates on solar air heaters with artificial S-shaped irregularity on the absorber plate. *Journal of Energy Storage, 74*, p. 109289. doi: 10.1016/j.est.2023.109289.

[9] Cyriac, B. and Bhusnoor, S.S., 2023, March. Performance Optimization of an Air Heater with Delta Flow Obstructions: A Taguchi Approach. *In Proceedings of International Conference on Intelligent Manufacturing and Automation: ICIMA 2022* (pp. 621-630). Singapore: Springer Nature Singapore.

[10] Rautela, M., Sharma, S.L., Bisht, V.S., Debbarma, A. and Bahuguna, R., 2023. Numerical Analysis of Solar Air Heater Roughened with B-Shape and D-Shape Roughness Geometry. *Journal of Heat and Mass Transfer Research, 10(1)*, pp. 101-120. doi: 10.22075/jhmtr.2023.30710.1445.

[11] Maithani, R., Chamoli, S., Kumar, A. and Gupta, A., 2019. Solar air heater duct roughened with wavy delta winglets: correlations development and parametric optimization. *Heat and Mass Transfer, 55(12)*, pp.3473-3491. doi: 10.1007/s00231-019-02651-9.

[12] Maithani, R., Silori, A., Rana, J. and Chamoli, S., 2017. Numerical analysis of heat transfer and fluid flow of a wavy delta winglets in a rectangular duct. *Thermal Science and Engineering Progress, 2*, pp.15-25. doi: 10.1016/j.tsep.2017.04.002.

[13] Sarreshtedari, A. and Zamani Aghaee, A., 2014. Investigation of the thermo-hydraulic behavior of the fluid flow over a square ribbed channel. *Journal of Heat and Mass Transfer Research, 1(2)*, pp. 107-115. doi: 10.22075/jhmtr.2014.186.

[14] Thapa, R.K., Bisht, V.S., Rawat, K.S. and Bhandari, P., 2022. Computational analysis of automobile radiator roughened with Rib roughness. *Journal of Heat and Mass Transfer Research, 9(2)*, pp.209-218. doi: 10.22075/jhmtr.2023.27617.1382.

[15] Dutta, P. and Dutta, S., 1998. Effect of baffle size, perforation, and orientation on internal heat transfer enhancement. *International Journal of Heat and Mass Transfer, 41(19)*, pp.3005-3013. doi: 10.1016/S0017-9310(98)00016-7.

[16] Karwa, R., Maheshwari, B.K. and Karwa, N., 2005. Experimental study of heat transfer enhancement in an asymmetrically heated rectangular duct with perforated baffles. *International Communications in Heat and Mass Transfer, 32(1-2)*, pp. 275-284. doi: 10.1016/j.icheatmasstransfer.2004.10.002.

[17] Cyriac, B. and Bhusnoor, S.S., 2023. Thermal and hydraulic characteristics of an air heater with modified delta flow obstructions. *e-Prime-Advances in Electrical Engineering, Electronics and Energy, 4*, p.100147. doi: 10.1016/j.prime.2023.100147.

[18] Cyriac, B. and Bhusnoor, S.S., 2023. Numerical investigation of heat transfer performance of an air heater with delta flow obstruction. *Materials Today: Proceedings, 72*, pp.1246-1252. doi: 10.1016/j.matpr.2022.09.295.

[19] Reddy, P.N., Verma, V., Kumar, A. and Awasthi, M.K., 2023. CFD Simulation and Thermal Performance Optimization of Flow in a Channel with Multiple Baffles. *Journal of Heat and Mass Transfer Research, 10*(2), pp. 257–268, 2023, doi: 10.22075/JHMTR.2023.31108.1458.

[20] Webb, R.L., Eckert, E.R.G. and Goldstein, R., 1971. Heat transfer and friction in tubes with repeated-rib roughness. *International journal of heat and mass transfer, 14(4)*, pp. 601-617. doi: 10.1016/0017-9310(71)90009-3.

[21] Han, J.C., Park, J.S. and Lei, C.K., 1985. Heat transfer enhancement in channels with turbulence promoters. *J. Eng. Gas Turbines Power 107(3)*, pp. 628–635. doi: 10.1115/1.3239782.

[22] Baissi, M.T., Brima, A., Aoues, K., Khanniche, R. and Moummi, N., 2020. Thermal behavior in a solar air heater channel roughened with delta-shaped vortex generators. *Applied Thermal Engineering, 165*, p. 113563. doi: 10.1016/j.applthermaleng.2019.03.134.

[23] Patankar, S.V., Liu, C.H. and Sparrow, E.M., 1977. Fully developed flow and heat transfer in ducts having streamwise-periodic variations of cross-sectional area. *J Heat Transfer, 99(2)*, pp. 180–186. doi: 10.1115/1.3450666.

[24] Tamna, S., Skullong, S., Thianpong, C. and Promvonge, P., 2014. Heat transfer behaviors in a solar air heater channel with

multiple V-baffle vortex generators. *Solar Energy*, 110, pp. 720-735. doi: 10.1016/j.solener.2014.10.020.

[25] Skullong, S., Promthaisong, P., Promvonge, P., Thianpong, C. and Pimsarn, M., 2018. Thermal performance in solar air heater with perforated-winglet-type vortex generator. *Solar Energy, 170*, pp.1101-1117. doi: 10.1016/J.SOLENER.2018.05.093.

[26] Yadav, A.S. and Thapak, M.K., 2014. Artificially roughened solar air heater: Experimental investigations. *Renewable and Sustainable Energy Reviews, 36*, pp. 370-411. doi: 10.1016/j.rser.2014.04.077.

[27] Aharwal, K.R., Gandhi, B.K. and Saini, J.S., 2008. Experimental investigation on heat-transfer enhancement due to a gap in an inclined continuous rib arrangement in a rectangular duct of solar air heater. *Renewable energy, 33(4)*, pp. 585-596. doi: 10.1016/j.renene.2007.03.023.

[28] Bekele, A., Mishra, M. and Dutta, S., 2014. Performance characteristics of solar air heater with surface mounted obstacles. *Energy conversion and management, 85*, pp.603-611. doi: 10.1016/j.enconman.2014.04.079.

[29] Bekele, A., Mishra, M. and Dutta, S., 2011. Effects of delta-shaped obstacles on the thermal performance of solar air heater. *Advances in Mechanical Engineering, 3*, p.103502. doi: 10.1155/2011/103502.

[30] Kumar, A. and Layek, A., 2022. Evaluation of the performance analysis of an improved solar air heater with Winglet shaped ribs. *Experimental Heat Transfer, 35(3)*, pp. 239-257. doi: 10.1080/08916152.2020.1838670.

[31] Jain, S.K., Agrawal, G.D., Misra, R., Verma, P., Rathore, S. and Jamuwa, D.K., 2019. Performance Investigation of a Triangular Solar Air Heater Duct Having Broken Inclined Roughness Using Computational Fluid Dynamics. *Journal of Solar Energy Engineering, 141(6)*, p.061008. doi: 10.1115/1.4043751.

[32] Karmare, S.V. and Tikekar, A.N., 2007. Heat transfer and friction factor correlation for artificially roughened duct with metal grit ribs. *International Journal of Heat and Mass Transfer, 50(21-22)*, pp.4342-4351. doi: 10.1016/j.ijheatmasstransfer.2007.01.065.

[33] Momin, A.M.E., Saini, J.S. and Solanki, S.C., 2002. Heat transfer and friction in solar air heater duct with V-shaped rib roughness on absorber plate. *International Journal of Heat and Mass Transfer, 45(16)*, pp.3383-3396. doi: 10.1016/S0017-9310(02)00046-7.